http://doi.org/10.35784/iapgos.5328 *received: 11.07.2023 | revised: 19.08.2023 | accepted: 05.09.2023 | available online: 30.09.2023*

RESEARCH THE EFFECT OF THE FRACTIONAL NUMBER SLOTS OF POLE ON WIND TURBINE GENERATION USING THE ENHANCED SPOTTED HYENA OPTIMIZATION ALGORITHM

Ibrahim M. Aladwan[1], Hasan Abdelrazzaq AL Dabbas[2], Ayman. M. Maqableh[3], Sayel M. Fayyad[4], Oleksandr Miroshnyk[5], Taras Shchur[6], Vadym Ptashnyk[7]

[1]Al-Balqa Applied University, Department of Mechatronics Engineering, Al Salt, Jordan, [2]Philadelphia University, Department of Mechanical Engineering, Amman, Jordan, [3]Luminus Technical University College, Electomechanical Engineering Department, Amman, Jordan, [4]Al-Balqa Applied University, Department of Mechanical Engineering, Al Salt, Jordan, [5]State Biotechnological University, Department of Electricity Supply and Energy Management, Kharkiv, Ukraine, [6]Cyclone Manufacturing Inc, Mississauga, Ontario, Canada, [7]Lviv National Environmental University, Department of Information Systems and Technologies, Lviv, Ukraine

Abstract. *The design of machines with permanent magnets is actively developing day by day and is often used in wind energy. The main advantages of such variable speed drives are high efficiency, high power density and torque density. When designing a wind generator with two rotors and permanent magnets, it is necessary to solve such a problem as the correct choice of the number of poles and slots to increase efficiency and minimize the cost of the machine. In this work, an improved spotted hyena optimization algorithm is used to obtain the optimal combination of slots and poles. This optimization algorithm makes it possible to obtain the number of fractional slots per pole and evaluate the operating efficiency of a wind generator with a double rotor and ferrite magnets. At the first stage of machine design, various combinations of slots are installed. Next, the optimal combination is selected from various slot-pole combinations, taking into account the Enhanced Spotted Hyena Optimization (ESHO) algorithm, in which a multi-objective function is configured. Accordingly, the multi-objectives are the integration of reverse electromotive force, output torque, gear torque, flux linkage, torque ripple along with losses. Analysis of the results obtained shows that the proposed algorithm for determining the optimal slot combination is more efficient than other slot combinations. It has also been found that the choice of slot and pole combination is critical to the efficient operation of permanent magnet machines.*

Keywords: wind turbine generation, optimal slot, pole, ESHO algorithm

BADANIE WPŁYWU UŁAMKOWEJ LICZBY SZCZELIN BIEGUNÓW NA GENERACJĘ TURBINY WIATROWEJ PRZY UŻYCIU ULEPSZONEGO ALGORYTMU OPTYMALIZACJI CĘTKOWANEJ HIENY

Streszczenie. *Projektowanie maszyn z magnesami trwałymi aktywnie rozwija się z dnia na dzień i jest często wykorzystywane w energetyce wiatrowej. Głównymi zaletami takich napędów o zmiennej prędkości są wysoka sprawność, wysoka gęstość mocy i gęstość momentu obrotowego. Podczas projektowania generatora wiatrowego z dwoma wirnikami i magnesami trwałymi konieczne jest rozwiązanie takiego problemu, jak prawidłowy dobór liczby biegunów i szczelin w celu zwiększenia wydajności i zminimalizowania kosztów maszyny. W niniejszej pracy zastosowano ulepszony algorytm optymalizacji hieny plamistej w celu uzyskania optymalnej kombinacji szczelin i biegunów. Ten algorytm optymalizacji umożliwia uzyskanie liczby ułamkowych szczelin na biegun i ocenę wydajności operacyjnej generatora wiatrowego z podwójnym wirnikiem i magnesami ferrytowymi. Na pierwszym etapie projektowania maszyny instalowane są różne kombinacje szczelin. Następnie wybierana jest optymalna kombinacja spośród różnych kombinacji szczelin i biegunów, biorąc pod uwagę algorytm Enhanced Spotted Hyena Optimization (ESHO) (ulepszony algorytm optymalizacjihieny cętkowanej hieny), w którym skonfigurowana jest funkcja wielocelowa. W związku z tym, celami wielozadaniowymi są integracja odwrotnej siły elektromotorycznej, wyjściowego momentu obrotowego, momentu obrotowego przekładni, połączenia strumienia, tętnienia momentu obrotowego wraz ze stratami. Analiza uzyskanych wyników pokazuje, że proponowany algorytm określania optymalnej kombinacji szczelin jest bardziej wydajny niż inne kombinacje szczelin. Stwierdzono również, że wybór kombinacji szczelin i biegunów ma kluczowe znaczenie dla wydajnej pracy maszyn z magnesami trwałymi.*

Słowa kluczowe: generacja turbiny wiatrowej, optymalna szczelina, biegun, algorytm ESHO

Introduction

Permanent magnet (PM) motors are intensively studied during the last few years [5, 13, 14, 19–21]. Presently, concerning the higher power/torque density along with high efficiency, fractional slot PM machines (FSPMMs) are extensively engaged in industrial automation, electrical vehicle and power generation including several other applications [14, 19, 21]. Basically, the PM machines (PMM) are modelled in a manner so that in contrast with the magnets, the air gap flux density (FD) regarding the armature reaction is lower. This will avert the PM's demagnetization in the event of defect currents in the stator windings [20]. Even though conventional fractional slot PMM having the entire teeth wound windings demonstrates better effectiveness, the coils localized at the final part of every single section could be effortlessly spoiled by simply being in the open air [5]. Alternatively, the high torque requisite on direct drive PM machines constantly results in a larger machine size together with material consumption [13]. PMMs have been broadly utilized in numerous applications. The PMMs are established as a generator in a wind turbine (WT) in the perspective of renewable energy systems [23, 27]. With specific reference to vehicle traction drives, and the direct-drive wind power generators, the consequence of fractional-slot of winding (FSCW) PMMs is concentrated broadly and is spotlighted here [25]. The entire functions necessitate high torque quality [12, 18]. Naturally, an electric machine is somewhat a conventionalist drive part that is improving slower than electronic components along with program control logic. This unit is the motor that verifies the drive's energetic data and also the weight-size parameters completely and to a great extent and that's why it is extremely essential to optimize this unit [8]. FEA software is utilized in the procedure of modelling the machine [24, 29, 30]. The well-known models of FEA tools are QuickField, Altair Flux, and as well FEMM. The first two models are proprietary software and the last model is free of software [31]. Rare-Earth (RE), also the non-RE, is the PM material's classification. Terbiums (Tb), Samarium (Sm), Dysprosium (Dy) along with Neodymium (Nd) are certain RE Elements (REEs) of RE-PMs. The two major categories of non-RE PMs are Alnico and Ferrite (Fe), which date to the earlier 1930s and 1950s, respectively [40]. Proportionate to the proficiency and the consistency, the PMSM could be preferred. The difficulties in PMSM are the high price and the flux's weakening on limiting the electric loading [22]. PMSMs could be organized as Surface-mounted PM Machines (SPMs) as well Interior PM Machines (IPMs) regarding the PM's positions [34]. The features and the proficiency of synchronous SPM machines are extremely exaggerated by the slot-pole combination [7]. The consequence of phase number on the winding factors, CT frequency and net radial forces are systematically scrutinized in various previous researches, which offers guiding principles to choosing the optimal slot/pole number combinations for multi-phase PMM [10]. The numeral count of stator slots per rotor poles per phase ratio directly influences

the PMSM's proficiency [1, 4, 33]. Subsequently, the foremost step in the PMM is selecting the slot-pole combinations. In this study, the outcome of the fractional number of SPP in PMM is being evaluated by choosing the slot-pole.

The authors of the article [33] evaluated the consequence of various pole-slots combinations on the generator's performance and at last established a set of methods that are comparatively better. The simulation outcomes validated that this methodology efficiently minimized the higher harmonic of no-load counter electromotive force in addition to that it enhanced the induced voltage distortion rate along with torque vibration and considerably enhanced the proficiency of the motor [37, 38]. And this scheme was utilized as the guiding signification for the structural optimization of superconducting motors.

In the paper [3] proffered a fresh modular fractional slot PMM having redundant teeth. The manufacturing of modular PMM with 42-slots/32-poles (42S/32P) combination was detailed elaborately like an instance, and that was handled as the amalgamation of six 6S/5P segments as well as a redundant 6S/2P device. Extra security was offered for coils positioned in these areas because the end part of every single section in the modular PMM was enclosed by half a redundant tooth in production. Progressively, the machine's fault-tolerant capacity was enhanced by the partition of six segments. By deploying the dual three-phase winding the modular machine's efficacy was improved and it was established by the electromagnetic performance fore-casted by FEA.

At paper [6] executed an absolute sensitivity exploration of the optimal parameters for the axial flux PM synchronous machines running in the field weakening (FW) area. The two design purposes of the methodology were to enlarge the power density (Power density is the ratio of fraction of maximal to rated speed: n_{max}/n_r and the associated inductance parameter maintaining the proficiency at the aimed speed beyond 90%) and to deliberate the optimal combination for every single phase, various slots/poles/phases combinations were deliberated. The outcome of the ratio of a number of stator slots to the number of rotor poles on the Power density and the nmax/nr was also calculated. It was exposed that the bettered Power density was attained by the factors having the low values. Regarding the "2" design goals, the outcome of the ratio of the outer diameter as well the inner to the outer diameter was illustrated. Consequently, the finite, also the theoretical infinite speed designs, were contrasted. The analytical design's potency was recognized by studying the entire 3D finite element (FE).

Autor of paper [35] proffered Fractional Slot PM (FSPM) machines by the fractional numbers of the slots for each part in a single periodicity of the machines. Alter-natively, the phase back-EMF signals were well-proportioned. Furthermore, the multi-layer winding methodology was deployed with the target of attaining a slot/pole com-bination by a small Unbalance Magnetic Force (UMF) also the armature MMRF's low THD value. Additionally, for discovering the multilayer winding's arrangement, a simple methodology was proffered by utilizing an extremely small UMF.

At work [15] examined the interior PM (IPM) machine's terminal voltage distortion by fractional slot concentrated windings (FSCW), also a specific prominence on the outcome of stator slot (Ns) together with rotor pole ($2p$) combinations. Initially, the 12-slot/10-pole machine was deployed for certifying the happening of voltage distortion. The methodology was then scrutinized by deploying the frozen permeability (FP) technique. The outcome of this examination exposed that the disparity in flux paths owing to rotor saliency was the cause of such a phenomenon, particularly whilst the present advancing angle reached 90°. Consequently, regarding the unavoidable device saturation, a design trade-off was utilized by choosing appropriate Ns/2p combinations for minimizing the effect. At last, for certifying the evaluation, prototypes were formulated.

In the paper [17] proffered an 18-slot/26-pole FSPM surface-mounted device (FSPMSM) having a coil-pitch of 2 slot-pitches. The machine's torque creation was done taking into account the fractional slot machine's principle together with the magnetic gear's outcome. Its proficiency was evaluated and correlated by an 18-slot/10-pole FSPMSM. The outcomes confirmed that the 18-slot/26-pole FSPMSM had better flux weakening capacity, smaller torque ripple, larger torque along with torque density, also a higher efficacy region in contrast to its 10-pole counterpart. Additionally, the possible slot/pole combinations of FSPMSMs having coil-pitch of 2 slot-pitches regarding the similar working rule were employed [2, 9, 36, 39].

1. Materials and methods

The PM generator that is directly operated by WT has the remunerations of higher efficiency, the simple structure and the reliable operation, also the characteristics of multi-pole, low speed, and large size. The disputes to be resolved while structuring a direct-driven PM wind generator are sufficient utilization of the structural dimension, enhancing the proficiency, and minimizing the machine's price by appropriate selection of the pole number and the Ns number [11, 16, 28]. The consequence of the fractional number of SPP and the optimal slot-pole combination in WT PMM is evaluated in this research. In the 1st phase, the wind generator and their magnetic pressure is obtained. Next, the slot-pole combination is initiated. Afterward, by deploying the ESHO algorithm the optimal slots along with poles combination are chosen. Figure 1 displays the present technique's block diagram [26, 41].

Fig. 1. Block diagram for the presented research [16]

1.1. Design of wind turbine generator

The WT is modelled to produce the highest power at a large spectrum of wind speeds. Nevertheless, during initialization, the significant model, and the decision in selecting the appropriate site meant for a WT. The WT's mechanical output power (O_p) is specified as

$$Q_p = \frac{1}{2}\rho\pi L^3 P_C(\omega,\delta)u_w^3 \tag{1}$$

The ω in equation (1) is the proportion of the blade tip's speed to the wind's speed which is expressed as

$$\omega = \frac{\eta_t L}{u_w} \tag{2}$$

where ρ – the air density in (kg/m^3); L – is the radius of the rotor's swept area (m); P_c – the power coefficient. This coefficient is a function of ω also the blade's pitch angle δ in (deg). The power coefficient is proffered as the division of the turbine mechanical power by the power accessed by the wind; u_w – the wind speed (m/sec); η_t – denotes the rotor angular speed (rad/sec) together with that the WT's aerodynamic mechanical torque (Mt) which is formulated as

$$M_t = \frac{\frac{1}{2}\rho\pi L^3 P_C(\omega,\delta)u_w^3}{\omega} \tag{3}$$

In DRPM wind generators, between 2 concentric rotors, the up stator is inserted, along with that the surface-mounted FM is extensively polarized in various directions. For that reason, the magnetic circuits in the DRPM wind generator's inner as well as in outer parts are in parallel, with that they divide up a common stator yoke. The circularly wounded winding is implemented, hence the insulation of the layer inside the slot isn't required having the benefits like less copper loss, easy maintenance, and as well short end winding. The fluxes flowing via the inner and the outer parts are similar, accordingly, the DRPM wind generator can be witnessed as an inner rotor generator occupied within an outer rotor one with single-layer winding.

In the DRPM WT generator, a magnetic pressure is deployed. As of the magnetic flux (MF) density, the electromagnetic pressure is measured utilizing the Maxwell stress tensor. The radial pressure brings out a vibration response, for this reason, the peripheral elements of the MF density are devalued. The radial pressure is formulated as:

$$R_r(\theta,t) \backsimeq \frac{\beta_r(\theta,t)}{2\gamma_0} \tag{4}$$

where β_r – denotes the radial MF regarding and its determined using the following expression

$$\beta_r(\theta,t) = \Lambda(\theta,t)F_r(\theta,t) \tag{5}$$

The MMF $F_r(\theta,t)$ is presented as

$$F_r(\theta,t) = \sum_{k=1}^{\infty} A_k \cos((\varepsilon_k t - kl\theta) \tag{6}$$

where θ – the tangential position; t – time; R_r – the radial pressure; γ_0 – the magnetic permeability of the air.

The MF is then obtained by multiplying the MMF by the air-gap permeance: $\Lambda_{slot}(\theta,t)$ – specifies the air-gap permeance; $F_r(\theta,t)$ – indicates the magnetomotive force (MMF); A_k – denotes the k-th MMF wave's amplitude; ε_k – the rotational frequency (rad/sec), which is $\varepsilon_k = k{\cdot}l{\cdot}v$ for the k-th harmonic; v – the rotor's rotational frequency (rad/sec); l – the number of pole pairs.

If the machine's slots are considered, the air-gap permeance variation pertained to the slots must be regarded, which is generally expressed by a Fourier series:

$$\wedge_{slot}\ (\theta,t) = \wedge_0 + \sum_{k=1}^{\infty} \wedge_h \cos(hS_2\theta) \tag{7}$$

So, the MF density is derived by substituting equation (7) in equation (5)

$$\beta_r(\theta,t)|_{ecc=\xi} = F_r(\theta,t)[\wedge_0 + \sum_{k=1}^{\infty} \wedge_h \cos(hS_2\theta)] \tag{8}$$

where h – the harmonic; S_2 – the number slots; Λ_0 – the air-gap permeance without slots; Λ_h – the coefficients of the Fourier series.

If the outcome of the slots is added, a novel spatial harmonic is attained consequently by the amalgamation of the MMF's harmonics and the slots. Consequently, the harmonics of spatial orders $k{\cdot}l \pm h{\cdot}s$ are attained, and the harmonics of the MMF of spatial order $k{\cdot}l$. In equation (4), the radial pressure is attained subsequently the MF's harmonics are added to and subtracted from one another for indicating the pressure's harmonics

1.2. Initialize the slot-pole combination

This stage initiates the number of slot-pole combinations. The number *SPP* per phase SPP_q is a fraction and not an integer, moreover this information is signified as "fractional slot winding". The total phases are denoted by *m*. The doubling-up of these phases is contrasted to a three-phase system that reduces *SPPq* into half. It relied upon the number of slots S_s and the number of pole pairs *l*.

$$SPP_q = \frac{S_s}{2lm} \tag{9}$$

A six-phase machine is nothing but an amalgamation of two three-phase systems. A division of the combinations to three-phase windings is the feasible combination of S_s and the number of poles 2*l*. In this work, the DRPM wind generator's slot as well the pole combination is selected like 12-slot/10-pole, 12-slot/14-pole, 18-slot/16-pole, 18-slot/20-pole, 24-slot/22-pole, and 24-slot/26-pole.

1.3. Optimal slot-pole combination selection using ESHO algorithm

Various slot-pole combinations are initiated and then by deploying the ESHO methodology the optimal slot-pole combination is elected. This selection process is very significant for developing the DRPM WT generator. Initially, the population is initiated. In this, the initial population is the slot-pole combination which is specified as (Z_i, i = 1, 2, 3, … n). The fitness is estimated after the initialization. The fitness is measured regarding the amalgamation of CT, EMF, OT, torque pulsation, FL and losses.

If the phase currents are zero a torque occurs between stator slots and rotor magnets, and this torque is termed CT. This influences vibrations, torque fluctuations, along with acoustic noise in the machine. The generator's proficiency as well as their lifetime may get reduced because of these negative features. Moreover, in WTs, the huge CT with low speed controls the rotor's rotation therefore the electricity production is prevented. Henceforth, in situations like this, the lessening of these effects is essential; by decreasing the CT's value. CT(J_{cog}) with the variables of rotor's position and air gap can be expressed mathematically with Equation:

$$I_{cog} = \frac{1}{2}\varpi_{air}^2 \frac{dw}{d\theta} \tag{10}$$

where w – the air gap reluctance; $\bar{\omega}_{air}$ – the air gap flux amount; θ – the rotor's position.

The CT's value is a function of the change in the air gap reluctance. The air gap value changes at regular intervals, subsequently, the CT's value changes as well. In this circumstance, CT is expressed with Fourier series and Equation:

$$I_{cog} = \sum_{k=1}^{\infty} J_{mk} \sin(hzk\theta) \tag{11}$$

where J_{mk} – the Fourier coefficient; h – the frequency; z – the least multiple of 2p number; k = 1, 2, 3 cycle number; θ – the rotor position.

Faraday's law of electromagnetic induction is deployed for assessing the back EMF in relation to the time variation of MF (12). Through the MF density (13) the MF is attained on the cross-section surface in the coil, which has to be vertical to the MF path

$$e_f = -N_t \frac{d\Omega}{dt} \tag{12}$$

$$\Omega = \iint BB_t ds \tag{13}$$

where e_f – back-electromotive force; N_t – the number of turns; $\frac{d\Omega}{dt}$ – the MF's time variation inside the coil; BB_t – the flux density.

While measuring the MF's time variation the constant angular velocity is being considered.

The complete power of the nacelle and the rotor hub must be favoured by the turbine tower, thus large PMGs are not desired in WT design. Nevertheless, the torque (and output power) may be augmented by other means. The sizing constant K is expressed as

$$K = \vartheta K_{wl}\left(a_{BB_t}\right)A_{ll} \tag{14}$$

where ϑ – the constant parameter; K_{wl} – the basic harmonic winding factor; a_{BB_t} – the rotor surface's average FD; A_{ll} – the electrical loading.

An unstable torque pulsation is formed by the CT's combination along with torque. Consequently, undesirable and additional vibrations along with noise have occurred while operating the machine. The mathematical derivation of torque pulsation J_p is

$$I_p = J_{cog} + J_{rip} \tag{15}$$

where J_{rip} – the torque ripple.

The interaction of a magnetic field with a material such as what would take place when a magnetic field goes via a coil of the wire causes FL. FL is proffered by the number of windings and the flux, where the instantaneous value of a time-varying flux is specified as $\vec{f}$. The $\vec{f}$ equation is specified as

$$\vec{f} = \overrightarrow{Nf} \tag{16}$$

where $\overrightarrow{Nf}$ – the total flux. In equation (17) the metrics combination is presented:

$$F_{it} = j_{cog} + e_f + K + J_p + PR_{gr} + \vec{f} \quad (17)$$

where F_{it} – the fitness function.

The encircling phase is processed after the fitness is being evaluated. Other searching factors will be considering their best position pertained to the prey or target as the best response and revise it. This action is mathematically given as:

$$A_y = \left|\Psi \cdot E_p(x) - \varsigma\left(E(x)\right)\right| \quad (18)$$

$$E_p(x+1) = E_p(x) - \tau \cdot A_y \quad (19)$$

where A_y – the distance between the spotted hyena and the prey; E_p – indicates the vector position pertained to the prey; E – the spotted hyena's vector position; x – the current iteration; ς – specifies the position vector's mean value that averts the convergence problem; ψ, τ – the coefficient factor vectors:

$$\Psi = 2 \cdot rand_1 \quad (20)$$

$$\tau = 2 \cdot g \cdot rand_2 - g \quad (21)$$

$$g = 5 - \left(Iteration \cdot \frac{s}{MAX_{Iteration}}\right) \quad (22)$$

g – the declines linearly from 5 to 0 to stabilize the exploration and the exploitation while having the maximum iterations in the process. This system enhances the development as the iterations $MAX_{iteration}$ increase. Where $rand_1$ and $rand_2$ are random vectors in [0, 1].

Next, the hunting process is executed. While hunting, the hyenas get information and the prey tracking capacity from their trusted friends. The hyena that has the finest statistics regarding the prey's position is proffered as the best search agent. Consequently, the best search agent is pursued by the other agents to revise their positions

$$A_y = \left|\Psi \cdot E_y - E_x\right| \quad (23)$$

$$E_k = E_y + E_{y+1} + \cdots E_{k+y} \quad (24)$$

$$I_k = E_k + E_{k+1} + \cdots E_{k+N} \quad (25)$$

where E_y – the spotted hyena's best position regarding the prey; E_k – together with this the spotted hyena's other position; N – the spotted hyena's total number, and then it is measured as:

$$N = Count_{nos}\left(E_y + E_{y+1} + \cdots E_{y+LO}\right) \quad (26)$$

LO – the denotes a random vector having a range of [0.5, 1]; nos – the count of answers, (the reference answers are counted); E_y – the group of N optimal answers.

Next, the attacking prey phase is processed. The vector value y is minimized for denoting the attacking prey mathematically. The differentiation in the vector τ is also minimized for changing the value in vector y which can lessen from 5 to 0 during iterations. The swarm of spotted hyenas hit the prey when $|\tau| < 1$. The attacking prey phase can mathematically be formulated as:

$$E(x+1) = \frac{I_y}{N} \quad (27)$$

where $E(x+1)$ – revises the other search agent's position to conclude the best search agent's position and the best solution.

The SHO algorithm permits its search agents to revise their positions and the attack towards the prey.

The search for prey is the closing phase. The exact answer is detected if $\tau \geq 1$, regarding equation (26). Vector ψ is the section of the SHO methodology where exploration is possible. Vector ψ holds random values that offer the prey's random weights regarding the equation (27). If the $\psi > 1$, vector has priority over the $\psi<1$ vector to display more random features of the SHO methodology and the distance's effect. Subsequently, the fitness value is being calculated. If the pre-specified threshold of the fitness value is not attained, then the process is continued till it attains the pre-specified threshold value. The optimal slot-pole combination is elected from the initialized slot-pole combinations by employing this methodology.

The pseudo-code for the ESHO methodology is represented in figure 2. In this pseudo-code, the initialization of the slot-pole combinations, fitness evaluation, and the updating procedure is given.

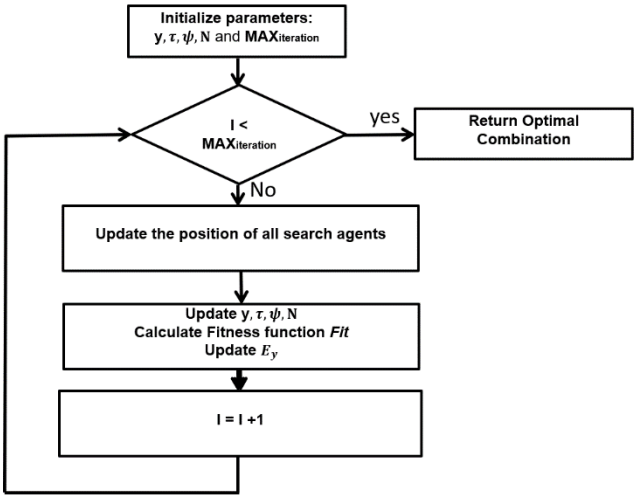

Fig. 2. Flow chart of the ESHO algorithm

2. Results and discussion

The slot-pole combination's effect is assessed in this section. MATLAB Simulink platform is deployed for executing the proffered work.

2.1. Performance analysis

Proportionate to the CT, FL, losses, back-EMF and OT; the usefulness of the optimal selection and without optimal slot-pole combination selection is evaluated. While considering the initialized slot-pole combination, a better slot-pole combination is attained in the optimal selection. And the average value of the entire initialized slot-pole combination was attained without optimal selection.

The FL analysis with optimal selection and without optimal selection is presented in figure 3. FL is small and takes place in electric machines. Flux lines take the path of least reluctance in most of the parts. Reluctance is proffered as the resistance to the flow of flux lines. These materials have a higher permeability. The number of slot-pole combination's optimal selection has less FL leakage than the slot-pole combinations without optimal selection. The evaluation is done regarding the variation in the rotor's position. If the rotor position is 180, the optimal selection has 0.4 Wb FL whereas without optimal selection it has 0.9 Wb. Accordingly, it points out that the optimal se-lection from the initialized slot-pole combination offers the finer result than the usual selection process.

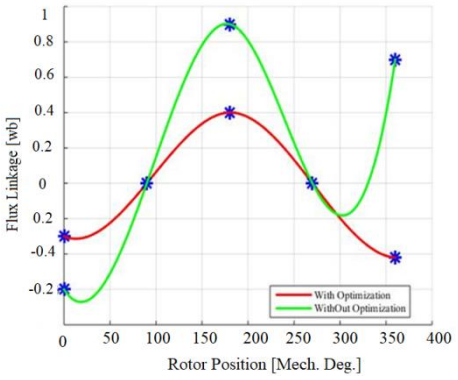

Fig. 3. FL analysis with optimal selection

CT of the slot-pole combination is presented in figure 4. It is significant to assess the CT. CT is one of the common challenges for machines. The harmonics in the back-EMF are pertained by the torque ripple in CT. Regarding the variation of the rotor position, the CT is evaluated. The optimal selection of slot-pole combination has less CT in correlation with the without

optimal selection option of the average value of the entire initialized slot-pole combination. For example, if the rotor position is 1, then with optimal selection-based slot-pole combination has 0.2 Nm whereas the without optimal selection has the 0.4 Nm. Correspondingly, for a range of rotor positions, with optimal selection has the finer outcome than the without optimal slot-pole combination.

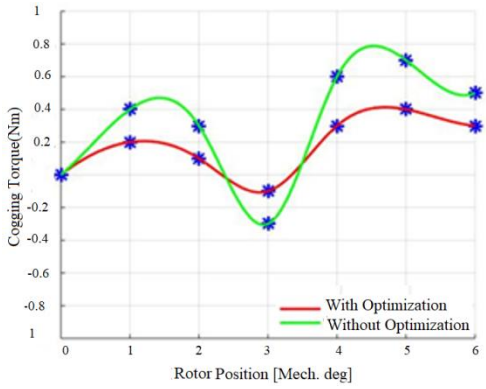

Fig. 4. Analysis of CT

The OT estimation of the slot-pole combination is assessed with optimum selection from the initialized slot-pole combination and the without optimal selection and then it is presented in figure 5. In general, the OT is centred on the rotor torque along with speed. Proportionate to the disparity in various electrical angles, the OT is evaluated. The model is specified as a better system if it has high OT. In this, the slot-pole combi-nation with optimal selection has higher OT than that without optimal selection. If the electrical angle is 360, with optimal selection has the 64 Nm OT and the without optimal selection has 43 Nm. The optimal slot-pole selection offers higher OT for the other electrical angles as well. Therefore, the best outcome is obtained using the recommended optimal selection.

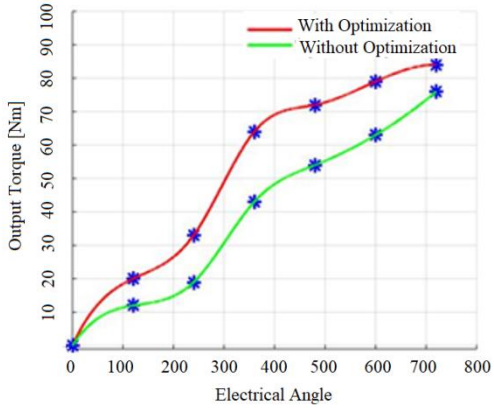

Fig. 5. Graphical representation of OT analysis

Figure 6 represents the losses regarding the slot-pole combination. The usefulness of the system and its reliability can be forecasted by having a better understanding of the features of the high-speed machine, particularly; a better understanding of its losses. The rotor losses could be high for high-speed machines, and in certain situations, these losses may harm the machine by the magnet's demagnetization. Hence, in machines, the assessment of losses is a major process. In relation to the rotor position angle, the loss is varied. In contrast, the with optimal slot-pole combination selection achieves lesser losses than the without optimal selection. For the rotor position 270, the optimal selection has 65 W whereas the without optimal slot-pole combination has the 78 W. A better result can also be obtained for the other rotor position by considering the with optimal slot-pole combinations.

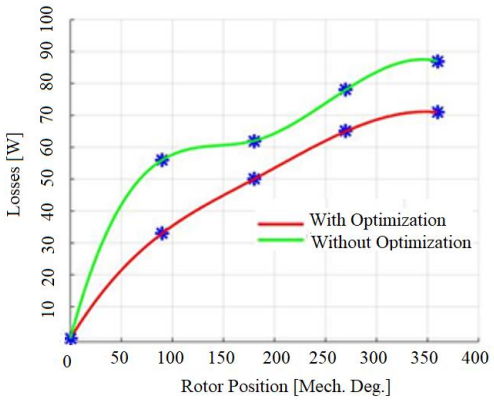

Fig. 6. Losses analysis

Figure 7 displays the Back-EMF of the slot-pole combination. In electric motors, the back EMF voltage occurs whilst there is a relative motion between the stator windings and the rotor's magnetic field. The figure of the back-EMF waveform is recognized by the rotor's geometrics features. In this, the efficiency is evaluated in relation to the rotors' position. For 180 rotor position, with optimal selection has 60 V whereas the without optimization has 80 V. Hence, a better proficiency is conquered with optimal selection.

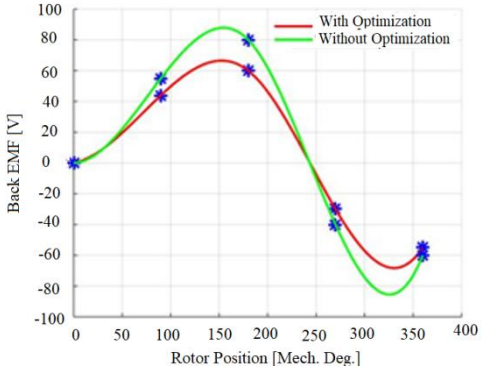

Fig. 7. Pictorial representation of the back-EMF analysis

The fitness vs iteration of the proffered ESHO methodology with the other methodologies, like SHO, Particle Swarm Optimization (PSO), Ant Colony Optimization (ACO), and Genetic Algorithm (GA) is represented in Fig. 8. For every single iteration, the fitness value varies. The proposed ESHO has 47 fitness for the 25th iteration. And for the same iteration, the fitness value for the previous methodologies is less than that of the proposed methodology. Likewise, for the 20th iteration, the ESHO has 34 fitness, whereas the previous methodologies have less fitness value than the proposed methodology. Subsequently, it is proved that a better outcome is achieved by the ESHO method-based selection than the without optimal selection and the other methods.

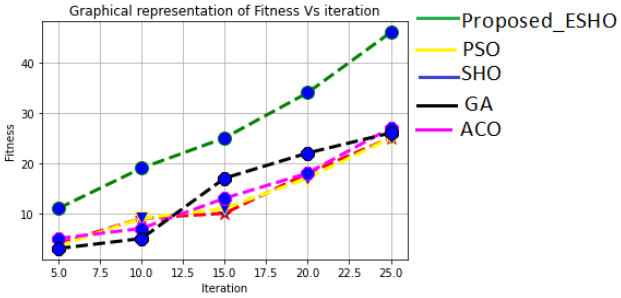

Fig. 8. Graphical representation of Fitness Vs iteration

3. Conclusions

The outcome of the SPP's fractional number in the DRPM WT generator with optimal slot-pole combination selection is assessed in this research. Mostly, small WTs utilize direct-driven PM generators, which have the characteristics of low speed and higher efficacy. Very simple controls are desired for small WTs as they are self-started. In the WT generator, the slot-pole combination obtains the main place and hence the significance of the SPP's fraction number. At first, the slot-pole combination is initialized and from that combination, the optimal selection is made by the ESHO. FLs, EMF, CT, OT, torque pulsation and losses are the features that are referred to during the selection process. The proficiency of the optimal slot-pole combination is evaluated with the entire initialized slot-pole combinations in relation to those factors. In this, the optimal selection of SPP's fraction number obtains better proficiency than the without optimal slot-pole combination selection. Thus, this method regarding the optimal slot-pole combination selection is crucial for the DRPM WT generator. In the future, the proposed methodology can be expanded by considering a variety of factors for a better optimal slot-pole combination selection.

References

[1] Abdelmoula R., Benhadj N., Chaieb M., Neji R.: Finite element comparative analysis software of a radial flux synchronous motor for electric vehicle drive. Proceedings of the International Conference on Recent Advances in Electrical Systems, 2016, 62–67.

[2] Al_Issa H. A., Qawaqzeh M., Khasawneh A., Buinyi R., Bezruchko V., Miroshnyk O.: Correct Cross-Section of Cable Screen in a Medium Voltage Collector Networkwith Isolated Neutral of a Wind Power Plant. Energies 14, 2021, 3026 [http://doi.org/10.3390/en14113026].

[3] Ambekar R., Ambekar S.: Design investigation for continual torque operative performance of PMSM for vehicle. Sādhanā 45, 2020, 120 [http://doi.org/10.1007/s12046-020-01360-y].

[4] Andrade K. M., Santos H. E., Wellington M. V., Almeida T. E., Paula G. T.: PeMSyn – a free matlab-femm based educational tool to assist the design and performance assessment of synchronous machines. Eletron. Poten., Fortaleza 25(2), 2020, 163–172 [http://doi.org/10.18618/REP.2020.2.0009].

[5] Chakir A., Tabaa M., Moutaouakkil F., Medromi H., Alami K.: Control System for a Permanent Magnet Wind Turbine Using Particle Swarm Optimization and Proportional Integral Controller. International Review of Automatic Control (IREACO) 13(5), 2020 [http://doi.org/10.15866/ireaco.v13i5.18482].

[6] Chen X., Wang J.: Magnetomotive force harmonic reduction techniques for fractional-slot non-overlapping winding configurations in permanent-magnet synchronous machines. Chinese Journal of Electrical Engineering 3(2), 2017, 103–113 [http://doi.org/10.23919/CJEE.2017.8048416].

[7] Demir Y., Yolacan E., El-Refaie A., Aydin M.: Investigation of Different Winding Configurations and Displacements of a Nine-Phase Permanent-Magnet-Synchronous Motor with Unbalanced AC Winding Structure. IEEE Transactions on Industry Applications 55(4), 2018, 3660–3670 [http://doi.org/10.1109/TIA.2019.2913156].

[8] Dutta R., Pouramin A., Rahman M.: A novel rotor topology for high-performance fractional slot concentrated winding interior machine. IEEE Transactions on Energy Conversion 36(2), 2020, 658–670 [http://doi.org/10.1109/TEC.2020.3030302].

[9] Edhah S., Alsawalhi J., Al-durra A.: Multi objective optimization design of fractional slot concentrated winding synchronous machines. IEEE Access 7, 2019, 162874–162882 [http://doi.org/10.1109/ACCESS.2019.2951023].

[10] Gandzha S., Sogrin A., Kiessh I.: The comparative analysis of electric machines with integer and fractional number of slots per pole and phase. Procedia Engineering 129, 2015, 408–414 [http://doi.org/10.1016/j.proeng.2015.12.137].

[11] Hemeida A., Taha M., Abdallh A., Vansompel H., Dupre L., Sergeant P.: Applicability of fractional slot axial flux synchronous machines in the field weakening region. IEEE Transactions on Energy Conversion 32(1), 2016, 111–121 [http://doi.org/10.1109/TEC.2016.2614011].

[12] Iegorov O., Iegorova O., Miroshnyk O., Savchenko O.: Improving the accuracy of determining the parameters of induction motors in transient starting modes. Energetika 66(1), 2020, 15–23 [http://doi.org/10.6001/energetika.v66i1.4295].

[13] Ismagilov F., Vavilov V., Yamalov I., Karimov R.: Fault-Tolerant Electric Motors with Permanent Magnets and Electromagnetic Shunting. International Review of Aerospace Engineering (IREASE) 13(2), 2020, 51–58 [http://doi.org/10.15866/irease.v13i2.17751].

[14] Kolsi H., Ben Hadj N., Chaieb M., Neji R.: Design of Permanent Magnet Synchronous Motor by Means of Power Density Optimization For e-Vehicle Applications. International Review on Modelling and Simulations (IREMOS) 15(3), 2022 [http://doi.org/10.15866/iremos.v15i3.21739].

[15] Li G., Ren B., Zhu Z.: Design guidelines for fractional slot multi-phase modular machines. IET Electric Power Applications 11(6), 2017, 1023–1031 [http://doi.org/10.1049/iet-epa.2016.0616].

[16] Li X., Zhu Z., Thomas A., Wu Z., Wu X.: Novel modular fractional slot machines with redundant teeth. IEEE Transactions on Magnetics 55(9), 2019, 1–10 [http://doi.org/10.1109/TMAG.2019.2918190].

[17] Liu Y., Zhu Z.: Electromagnetic performance comparison of 18-slot/26-pole and 18-slot/10-pole fractional slot surface-mounted machines. 20th International Conference on Electrical Machines and Systems (ICEMS) 2017, 11–14 [http://doi.org/10.1109/ICEMS.2017.8056383].

[18] Liu Y., Zhu Z.: Influence of gear ratio on the performance of fractional slot concentrated winding machines. IEEE Transactions on Industrial Electronics 66(10), 2019, 7593–7602 [http://doi.org/10.1109/TIE.2018.2885728].

[19] Lounthavong V., Sriwannarat W., Seangwong P., Siritaratiwat A., Khunkitti P.: Optimal Stator Design to Improve the Output Voltage of the Novel Three-Phase Doubly Salient Permanent Magnet Generator. International Journal on Energy Conversion (IRECON) 8(4), 2020, 118–125 [http://doi.org/10.15866/irecon.v8i4.19302].

[20] Makhad M., Zazi K., Zazi M., Loulijat A.: Smooth Super Twisting Sliding Mode Control for Permanent Magnet Synchronous Generator Based Wind Energy Conversion System. International Journal on Energy Conversion (IRECON) 8(5), 2020, 171–180 [http://doi.org/10.15866/irecon.v8i5.19362].

[21] Murali N., Mini V. P., Ushakumari S.: Modified V-Shaped Interior Permanent Magnet Synchronous Motor Drive for Electric Vehicle. International Review on Modelling and Simulations (IREMOS) 14(6), 2021 [http://doi.org/10.15866/iremos.v14i6.20884].

[22] Nur T., Mawar S.: Improvement of Cogging Torque Reduction by Combining the Magnet Edge Shaping and Dummy Slot in Stator Core of Fractional Slot Number in Permanent Magnet Machine. IOP Conference Series Materials Science and Engineering 807(1), 2020, 012023, 29–30 [http://doi.org/10.1088/1757-899X/807/1/012023].

[23] Ouiddir F., Benouzza N., Gherabi Z.: Stator Current Square Analysis to Discriminate Between Eccentricity and Demagnetization Faults in PMSMs. International Review of Electrical Engineering (IREE) 17(1), 2022, 11–19 [http://doi.org/10.15866/iree.v17i1.20950].

[24] Pazyi V., Miroshnyk O., Moroz O., Trunova I., Savchenko O, Halko S.: Analysis of technical condition diagnostics problems and monitoring of distribution electrical network modes from smart grid platform position. IEEE KhPI Week on Advanced Technology (KhPIWeek), 2020, 20168725, 57–60 [http://doi.org/10.1109/KhPIWeek51551.2020.9250080].

[25] Peng B., Wang X., Zhao W., Ren J.: Study on shaft voltage in fractional slot machine with different pole and slot number combinations. IEEE Transactions on Magnetics 55(6), 2019, 1–5 [http://doi.org/10.1109/TMAG.2019.2898566].

[26] Pezhman J., Taghipour S., Khoshtarash J.: Expansion of the feasible slot pole combinations in the fractional slot PM machines by applying three-slot pitch coils. IEEE Transactions on Energy Conversion 34(2), 2018, 993–999 [http://doi.org/10.1109/TEC.2016.2614011].

[27] Qawaqzeh M., Szafraniec A., Halko S., Miroshnyk O., Zharkov A.: Modelling of a household electricity supply system based on a wind power plant. Przegląd Elektrotechniczny 96, 2020, 36–40 [http://doi.org/10.15199/48.2020.11.08].

[28] Qawaqzeh M., Zaitsev R., Miroshnyk O., Kirichenko M., Danylchenko D., Zaitseva L.: High-voltage DC converter for solar power station. International journal of power electronics and drive system 11(4), 2020, 2135–2144 [http://doi.org/10.11591/ijpeds.v11.i4.pp2135-2144].

[29] Røkke A., Nilssen R.: Analytical calculation of yoke flux patterns in fractional-slot machines. IEEE Transactions on Magnetics 53(4), 2017, 1–9 [http://doi.org/10.1109/TMAG.2016.2623583].

[30] Savchenko O. A., Miroshnyk O. O., Dyubko S., Shchur T., Komada P., Mussabekov K.: Justification of ice melting capacity on 6-10 kV OPL distributing power networks based on fuzzy modeling. Przeglad Elektrotechniczny 95(5), 2019, 106–109.

[31] Shen J., Wang C., Miao D., Jin M., Shi D., Wang Y.: Analysis and optimization of a modular stator core with segmental teeth and solid back iron for pm electric machines. IEEE International Electric Machines & Drives Conference (IEMDC), 2011, 1270–1275 [http://doi.org/10.1109/IEMDC.2011.5994787].

[32] Szafraniec A., Halko S., Miroshnyk O., Figura R., Zharkov A., Vershkov O.: Magnetic field parameters mathematical modelling of windelectric heater. Przeglad elektrotechniczny 97(8), 2021, 36–41.

[33] Tahanian H., Aliahmadi M., Faiz J.: Ferrite Permanent Magnets in Electrical Machines: Opportunities and Challenges of a Non-Rare-Earth Alternative. IEEE Transactions on Magnetics 56(3), 2020, 1–20 [http://doi.org/900120.10.1109/TMAG.2019.2957468].

[34] Tessarolo A., Mezzarobba M., Barbini N.: Improved four-layer winding design for a 12-slot 10-pole machine using unequal tooth coils. 42nd Annual Conference of the IEEE Industrial Electronics Society – IECON 2016, 1686–1691 [http://doi.org/10.1109/IECON.2016.7793399].

[35] Torreggiani A., Bianchini C., Davoli M., Bellini A.: Design for Reliability: The Case of Fractional-Slot Surface Permanent-Magnet Machines. Energies 12, 2019, 1691 [http://doi.org/10.3390/en12091691].

[36] Torrent M., Perat J. I., Jiménez J. A.: Permanent Magnet Synchronous Motor with Different Rotor Structures for Traction Motor in High Speed Trains. Energies 11, 2018, 1549 [http://doi.org/10.3390/en11061549].

[37] Trunova I., Miroshnyk O., Savchenko O., Moroz O.: The perfection of motivational model for improvement of power supply quality with using the one-way analysis of variance. Naukovyi Visnyk Natsionalnoho Hirnychoho Universytetu 6, 2019, 163–168 [http://doi.org/10.29202/nvngu/2019-6/24].

[38] Tymchuk S., Miroshnyk O.: Assess electricity quality by means of fuzzy generalized index. Easternt-European Journal of enterprise technologies 3/4(75), 2015, 26–31 [http://doi.org/10.15587/1729-4061.2015.42484].

[39] Wang Q., Li Y., Deng G., Zhang H., Li Y., Xu J., Wang X.: Optimization Study of Poles-Slots Combination of Large Capacity Offshore HTS Wind Generator Based on Ansys Maxwel. Journal of Physics Conference Series 1754, 2021, 012042 [http://doi.org/10.1088/1742-6596/1754/1/012042].

[40] Zhu Z., Wu D., Ge X.: Investigation of voltage distortion in fractional slot interior machines having different slot and pole number combinations. IEEE Transactions on Energy Conversion 31(3), 2015, 1192–1201 [http://doi.org/10.1109/TEC.2016.2553140].

[41] Zou T., Qu R., Li D., Jiang D.: Synthesis of fractional-slot vernier permanent magnet machines. International Conference on Electrical Machines (ICEM) 2016, 911–917 [http://doi.org/10.1109/ICELMACH.2016.7732634].

Ph.D. Eng. Ibrahim M. Aladwan
e-mail: Ibrahim.aladwan@bau.edu.jo

Since 2014 he has been working at AL Balqa Applied University, Mechatronics Engineering Department as instructor for several courses related with Mechatronics Engineering. Dr. Ibrahim occupied several administrative positions, including Dean of Student Affairs, and Director of NTTI (National Training of Trainees Institute). In addition, Dr. Aladwan has a comprehensive training experience. His research interests include: Electric Drive, CNC machine, Renewable Energy.

http://orcid.org/0000-0002-7305-2413

Ph.D. Eng. Hasan Abdelrazzaq AL Dabbas
e-mail: drdabbas@engineer.com

Since 2014 he has been working at Philadelphia University, Faculty of Engineering, Department of Mechanical Engineering as instructor for several courses related with mechanical Engineering.
His research interests include: Materials Engineering, Mechanical Engineering Manufacturing Engineering, Mechanical Behavior of Materials Machining CNC Machining.

http://orcid.org/0000-0003-1301-4279

Ph.D. Eng. Ayman. M. Maqableh
e-mail: a.maqableh@ltuc.com

Maqableh has a Ph.D. in Mechanical Engineering from the University of Nottingham, UK. He has extensive experience in workforce development, technical and vocational education and public-private partnerships. He is currently the Dean of LTUC College-Jordan, managing more than 300 academic and administrative employees.

http://orcid.org/0000-0003-1301-4279

Ph.D Eng. Sayel M. Fayyad
e-mail: fswes@bau.edu.jo

Sayel M. Fayyad, holding Ph.D. in mechanical engineering, and B.A., Master degrees in mechanical engineering, computer science, education technology, and MBA, B.Sc. in mechanical engineering, physics and computer science. About 80 publications, working in Al-Balqa Applied University, Al Salt, Jordan since 2007 till now. Research work: control systems, vibrations, renewable energy and dynamics.

http://orcid.org/0000-0002-7305-2413

D.Sc. Eng. Oleksandr Miroshnyk
e-mail: omiroshnyk@btu.kharkiv.ua

Graduated from Kharkiv State Technical University of Agriculture, Kharkiv, Ukraine, in 2004, and was qualified as an Electrical Engineer. He received his Ph.D. in electric engineering (power stations, systems and networks) from the National Technical University "Kharkiv Politechnic Institute", Ukraine, in 2009 and Doctor of Technical Sciences degree in 2016.
His research interests are related to research in the field of smart grid, renewable energy and computer numerical control machines.

http://orcid.org/0000-0002-6144-7573

Ph.D. Eng. Taras Shchur
e-mail: shchurtg@gmail.com

Graduated from Kharkiv State Technical University of Agriculture, Kharkiv, Ukraine, in 2004, and was qualified as an mechanical engineer. He received his Ph.D. in mechanical engineering (Machines and means of mechanization of agricultural production) from the Kharkiv State Technical University of Agriculture, in 2009. His research interests are related to research in the field of smart grid, renewable energy and computer numerical control machines.

http://orcid.org/0000-0003-0205-032X

Ph.D. Vadym Ptashnyk
e-mail: ptashnykproject@gmail.com

Graduated from Lviv Polytechnic National University, Ukraine, in 2010, and was qualified as an applied physicist. He received his Ph.D. in ecological safety from the Sumy State University, Ukraine, in 2014.
His research interests are related to research in the field of Internet of Things, microprocessing technology and water quality control methods.

http://orcid.org/0000-0002-1018-1138